

Energy barriers to viscous flow and the prediction of glass transition temperatures of molten silicates

MICHAEL J. TOPLIS*

Centre de Recherches Pétrographiques et Géochimiques, Centre National de la Recherche Scientifique, BP20, F-54501 Vandoeuvre-lès-Nancy, France

ABSTRACT

Within the framework of the Adam-Gibbs (configurational entropy) theory of viscosity, it is shown that for a given composition, the ratio of parameters B_e (a temperature independent constant) to $S_c(T_g)$ (the configurational entropy at the glass transition) is proportional to the height of the average potential energy barrier to viscous flow ($\Delta\mu$) and the size of the rearranging domains at the glass transition [$z^*(T_g)$]. The ratio $B_e/S_c(T_g)$ is evaluated for several silicate and aluminosilicate compositions of variable polymerization. It is found that the ratio $B_e/S_c(T_g)$ shows simple compositional variations that correspond closely to those that may be expected qualitatively for the height of the potential energy barrier to viscous flow. Assuming that $z^*(T_g)$ is a constant for all compositions, the available data for $B_e/S_c(T_g)$ are parameterized as a function of $\Delta\mu$. The physical basis of this parameterization will therefore allow extension to more complex systems as additional data become available. The A_e term in the Adam-Gibbs equation (another temperature independent constant) shows only minor compositional variation (-2.6 ± 1), but the variation that does exist is found to be a linear function of $B_e/\text{tetrahedron}$. The proposed parameterizations of $B_e/S_c(T_g)$ and A_e are shown to be sufficient for estimating the glass transition temperature to within 15–20 K. Calculated glass transition temperatures may be combined with existing models for viscosities in the range $10\text{--}10^5$ Pa-s. Interpolation provides the whole viscosity curve and thus also an estimate of the departure from Arrhenian behavior. Although further work is necessary to verify and extend the parameterizations to compositions of direct geological relevance, this work represents a step toward a fully generalizable predictive model of silicate melt viscosity based within a physical framework.

INTRODUCTION

The ability to estimate silicate melt viscosity reliably is fundamental for understanding and predicting diverse processes of interest to the geological and applied sciences, such as convection in crustal magma chambers, melt migration in the mantle, the nature of explosive volcanism, or the transport of melts used for glass making, metallurgy, and waste disposal. The compositional and temperature ranges of interest to both geological and applied disciplines are very large, making direct viscosity measurements of all the compositions of interest impossible. This has led to various attempts at predictive models that, for compositions of geological interest, have been reasonably successful at temperatures well above the glass transition (Bottinga and Weill 1972; Shaw 1972). However, these empirical models do not take into account departures from Arrhenian behavior (an important characteristic of silicate melts, e.g., Richet 1984; Richet and Bottinga 1995) and are thus of little use at temperatures

close to the glass transition. In contrast to these empirical approaches, three other approaches (configurational entropy theories, Adam and Gibbs 1965; free-volume theories, Cohen and Grest 1979; and mode coupling theory, Götze 1991) have attempted to link quantitatively viscous relaxation time to some structural property of the melt. Of these three, the Adam-Gibbs (configurational entropy) theory can account for the non-Arrhenian behavior quantitatively as well as several other properties of a wide range of silicate compositions. (For further details of the theory and its application to silicate melts the reader is referred to Richet 1984 and Bottinga and Richet 1996).

In summary, the Adam-Gibbs (A-G) theory (Adam and Gibbs 1965; Richet 1984) relates viscosity (η) to absolute temperature (T) and the configurational entropy of the system at that temperature [$S_c(T)$] through the relation:

$$\log_{10} \eta(T) = A_e + B_e/TS_c(T) \quad (1)$$

where A_e and B_e are temperature independent constants (Richet 1984). The configurational entropy is not, however, a constant at all temperatures, and it is indeed the

* E-mail: mtoplis@cprg.cnrs-nancy.fr

temperature dependence of this term that results in non-Arrhenian behavior. At a given temperature above the glass transition the configurational entropy of the melt is:

$$S_c(T) = S_c(T_g) + \int_{T_g}^T C_p^{\text{conf}}/T dT \quad (2)$$

where $S_c(T_g)$ is the configurational entropy of the melt at the glass transition temperature, and C_p^{conf} is the configurational heat capacity of the melt phase (i.e., $C_p^{\text{melt}(T)} - C_p^{\text{glass}(T_g)}$). Strong evidence in favor of the application of the A-G theory to silicate melts is provided by the fact that values of $S_c(T_g)$ estimated from viscosity curves agree well with values of this parameter obtained independently by appropriate calorimetric cycles of relevant glass and crystalline materials (e.g., Richet 1984; Botttinga et al. 1995).

Despite the numerous demonstrations that the Adam-Gibbs theory successfully describes the temperature dependence of silicate melt viscosity, the theory has not been used in a predictive sense because of a lack of adequate models to describe the compositional variation of the parameters A_e , B_e , and $S_c(T_g)$. Calculation schemes for C_p^{conf} , on the other hand, do exist for a wide range of silicate compositions (Richet and Botttinga 1985, 1986). Hummel and Arndt (1985) and Tauber and Arndt (1987) assumed A_e and B_e to be linear functions of composition along the anorthite-albite and anorthite-diopside binaries, but the results of Tauber and Arndt (1987) as well as the data of Neuville and Richet (1991) suggest that such an assumption is probably not valid, as clearly illustrated in Figure 1 for the binary join CaSiO_3 - MgSiO_3 (Neuville and Richet 1991). Before describing the compositional dependence of each of these terms it is instructive to consider their physical significance, to interpret their variations within the framework of a physical model.

PHYSICAL SIGNIFICANCE OF A-G PARAMETERS

A_e

Although Adam and Gibbs (1965) did not discuss the physical significance of the A_e term in detail, an analogy may be made with kinetic theory (the Adam-Gibbs theory being a molecular-kinetic theory). In the case of a reaction that takes place through a single thermally activated process with an activation enthalpy ΔH_a and activation entropy ΔS_a , it may be shown (e.g., Putnis 1992) that the rate of reaction is:

$$\text{rate} = \nu \exp \{ \Delta S_a/R \} \exp \{ -\Delta H_a/RT \} \quad (3)$$

where ν is the frequency with which atoms attempt to partake in the reaction, R is the gas constant, and T is absolute temperature. In the case of viscosity the "reaction rate" is inversely proportional to τ , the relaxation time. Therefore, using the Maxwell relation ($\tau = \eta/G_\infty$; Dingwell and Webb 1989), it may be shown that:

$$\log \eta = \log G_\infty - \log \text{rate} \quad (4)$$

where G_∞ is the infinite frequency (unrelaxed) bulk modulus. Combining Equations 3 and 4 gives:

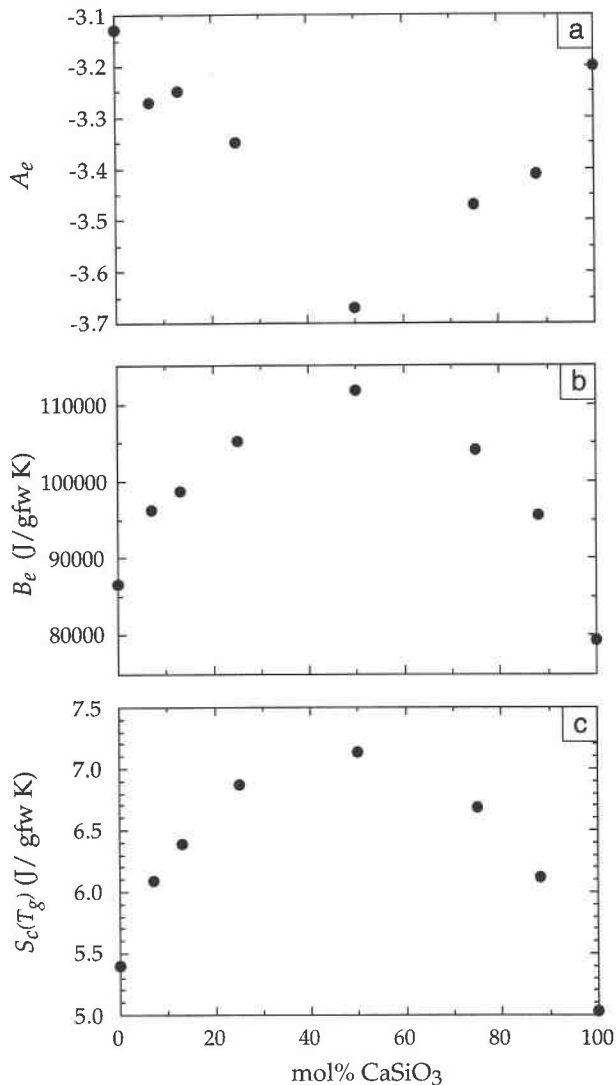


FIGURE 1. Variation of (a) A_e , (b) B_e , and (c) $S_c(T_g)$ for the system CaSiO_3 - MgSiO_3 (Neuville and Richet 1991; values per gram formula weight) showing the highly non-linear variation of these parameters, even in compositionally simple joins of constant polymerization.

$$\log \eta = \log G_\infty - \log \nu - \Delta S_a/2.303 R + \Delta H_a/2.303 RT \quad (5)$$

Therefore, the sum of the temperature independent terms, A_e , is:

$$A_e = \log G_\infty - \log \nu - \Delta S_a/2.303 R \quad (6)$$

For molten silicates, $\log G_\infty$ has a relatively constant value ($\log G_\infty = 10 \pm 0.5$; Dingwell and Webb 1989, 1990). As discussed by Dingwell and Webb (1989), the frequency ν may be expected to be on the same time scale as the "vibration of the liquid quasi-lattice" at infinite temperature, and thus also relatively constant for silicate compositions, in the range 10^{13} - 10^{14} Hz. Activation entropies should be similar in magnitude to $2.303 R$, thus the vari-

ation in A_e may be expected to be less than ± 2 for different molten silicates.

B_e

The B_e term is commonly considered analogous to the activation energy in an Arrhenian model of viscous flow. Indeed, B_e is related to the potential energy barrier to viscous flow, but is not equal to it as is often assumed. Adam and Gibbs (1965) showed that its magnitude is given by:

$$B_e = n_p \Delta\mu s_c^*/k \quad (7)$$

where n_p is the total number of particles in the system, $\Delta\mu$ is the average potential energy barrier to structural rearrangement, s_c^* is the configurational entropy of the smallest rearranging unit, and k is Boltzmann's constant. The observation that a single value for B_e may be fit to the viscosity curve of a silicate melt whose heat capacity is known (Richet 1984; Bottinga and Richet 1996) therefore implies that all of the terms on the right hand side of Equation 7 have a negligible temperature dependence. This in turn implies that the microscopic mechanism (or mechanisms) controlling viscous flow in a given melt does not change in its average energy barrier to rearrangement, or average entropy of the smallest rearranging units, at least in the range 10 – 10^{12} Pa·s, over which the A-G theory has been shown to be applicable (Bottinga et al. 1995). Although one may expect the height of the potential energy barrier to viscous flow to be a simple function of composition, it is very likely that the configurational entropy of the smallest rearranging unit will not show linear variations as a function of composition, a fact that may be responsible for variations in B_e such as those shown in Figure 1.

$S_c(T_g)$

Due to a lack of knowledge concerning the details of the relation between compositional factors and configurational entropy quenched in at the glass transition [$S_c(T_g)$], no model currently exists for the calculation of this parameter. However, the macroscopic configurational entropy at any temperature must be the sum of the configurational entropy of the units of which the melt is composed, and of which the smallest ones dominate (see discussion in Adam and Gibbs 1965). At the glass transition, this may be expressed as:

$$S_c(T_g) = N_t(T_g) s_c^* \quad (8)$$

where $N_t(T_g)$ is the total number of subsystems at the glass transition temperature (subsystem refers to the "smallest region that can undergo a transition to a new configuration without a requisite simultaneous configurational change on or outside its boundary," see Adam and Gibbs 1965, p. 141; cf. Bottinga and Richet 1996). With increasing temperature above the glass transition it is inferred that s_c^* is approximately constant (because B_e is temperature independent), but the number of subsystems gets larger with increasing temperature, thus leading

to an increase in the configurational entropy of the macroscopic system.

The ratio $B_e/S_c(T_g)$ and prediction of T_g

Even though calculation of both B_e and $S_c(T_g)$ requires estimation of the configurational entropy of the smallest rearranging units in the melt (s_c^*), it is clear from Equations 7 and 8 that their ratio does not (Eq. 9).

$$B_e/S_c(T_g) = \{n_p/N_t(T_g)\} \cdot \{\Delta\mu/k\} \quad (9)$$

The value of $n_p/N_t(T_g)$ is independent of the quantity of melt considered (and thus the definition of one mole of melt) and is in fact equal to the number of particles per smallest rearranging unit, i.e., the size of the rearranging units or z^* in the terminology of Adam and Gibbs (1965). Therefore we have the general equation

$$B_e/S_c(T_g) = z^*(T_g) \Delta\mu/k \quad (10)$$

that shows that variations in the ratio $B_e/S_c(T_g)$ may be due to changes either in the size of the smallest rearranging units at the glass transition [$z^*(T_g)$] or changes in the height of the average potential energy barrier to viscous flow ($\Delta\mu$).

The ratio $B_e/S_c(T_g)$ is of interest because it is a necessary parameter for the calculation of the glass transition temperature (T_g). If T_g is assumed to occur at the 10^{12} Pa·s viscosity isokom (an assumption that is supported by calorimetric measurements performed at laboratory cooling rates for a wide range of silicate compositions, see Richet and Bottinga 1995), then rearrangement of Equation 1 shows that:

$$T_g = B_e/S_c(T_g) \cdot 1/(12 - A_e) \quad (11)$$

Thus, the ability to predict: (1) the ratio $B_e/S_c(T_g)$, and (2) the parameter A_e permits the calculation of T_g .

COMPOSITIONAL VARIATION OF $B_e/S_c(T_g)$

Using data from the literature, the compositional dependence of the ratio $B_e/S_c(T_g)$ for the following simple silicate and aluminosilicate compositions will be considered: (1) fully polymerized network liquids, (2) sodium silicates, (3) alkali tetrasilicates, (4) the joins CaSiO_3 - MgSiO_3 and $\text{Ca}_3\text{Al}_2\text{Si}_3\text{O}_{12}$ - $\text{Mg}_3\text{Al}_2\text{Si}_3\text{O}_{12}$, and (5) the system Na_2O - CaO - SiO_2 .

Fully polymerized "network" liquids

SiO_2 , the compositionally simplest silicate system, is generally considered to consist of a fully polymerized network of silicate tetrahedra with the vast majority of O atoms playing "bridging" roles. Richet (1984) used the viscosity data of Urbain et al. (1982) and the calorimetric data of Richet et al. (1982) to report a set of Adam-Gibbs parameters for SiO_2 melt that give a value for $B_e/S_c(T_g)$ of 16 700 (Table 1). Below 1600 K, however, the viscosity data of Hetherington et al. (1964) diverge significantly from those of Urbain et al. (1982). As discussed by Richet (1984), the former measurements may have been affected by sample impurities whereas some doubt exists

TABLE 1. Summary of Adam-Gibbs parameters

	A_e	B_e J/gfw·K*	$S_{\alpha(T_g)}$ J/gfw·K*	$B_e/S_{\alpha(T_g)}$
SiO ₂ †	0.12	85 000	5.10	16 667
SiO ₂ ‡	-1.45	99 980	5.10	19 604
Alb§	-2.45	145 800	9.45	15 429
Alb	-2.45	137 520	8.72	15 771
Jad§	-2.52	141 000	9.52	14 811
Jad	-2.32	117 010	7.43	15 748
Neph§	-2.38	116 100	7.51	15 459
Neph	-2.51	120 470	7.66	15 727
An†	-2.08	140 800	9.20	15 304
Or†	-2.12	114 600	7.08	16 186
Na0.15#	-2.55	136 840	12.22	11 198
Na0.2†	-1.87	102 340	9.83	10 411
Na0.25#	-1.77	74 820	7.36	10 166
Na0.25†	-1.63	82 850	8.23	10 067
Na0.3#	-1.76	71 450	7.12	10 035
Na0.33†	-1.73	77 970	7.95	9 808
Na0.35#	-1.91	79 770	8.03	9 934
Na0.4#	-2.33	86 970	8.72	9 974
Na0.45#	-2.62	84 750	8.47	10 006
Wo 0**	-3.13	86 600	5.40	16 037
Wo 7**	-3.27	96 200	6.10	15 770
Wo 13**	-3.25	98 650	6.39	15 438
Wo 25**	-3.35	105 300	6.87	15 328
Wo 50**	-3.67	111 700	7.14	15 644
Wo 75**	-3.47	104 150	6.69	15 568
Wo 88**	-3.41	95 600	6.13	15 595
Wo 100**	-3.20	79 450	5.04	15 764
Gr 0**	-2.63	123 230	8.07	15 270
Gr 25**	-2.78	141 290	9.38	15 063
Gr 50**	-2.78	141 560	9.39	15 076
Gr 75**	-2.61	132 970	8.84	15 042
Gr 100**	-2.03	104 060	7.02	14 823
N25CS70††	-1.68	66 580	6.46	10 307
N20CS70††	-1.80	69 230	6.37	10 868
N15CS70††	-1.75	64 910	5.68	11 428
N10CS70††	-2.33	82 390	6.54	12 598
N5CS65††	-1.74	69 370	6.84	10 142
N10CS65††	-1.84	72 850	6.88	10 589
N15CS65††	-1.88	73 300	6.60	11 106
N20CS65††	-2.07	76 930	6.48	11 872

* gfw = gram formula weight.

† Parameters taken from Richet (1984). An = CaAl₂Si₂O₈; Or = KAlSi₃O₈.

‡ Parameters calculated using the viscosity data of Hetherington et al. (1964) for temperatures below 1600 K and the calorimetric data of Richet et al. (1982).

§ Parameters taken from Toplis et al. (1997a) for compositions exactly along the join SiO₂-NaAlSi₃O₆. Alb = NaAlSi₃O₈; Jad = NaAlSi₂O₆; Neph = NaAlSiO₄.

|| Parameters calculated using the viscosity data of Toplis et al. (1997a) for compositions close to the join SiO₂-NaAlSiO₄ and containing no non-bridging O atoms.

Parameters calculated using the viscosity data of Knoche et al. (1994) and the model of Richet and Bottinga (1985) for values of C_p^{cont} . Na_x corresponds to $x\text{Na}_2\text{O}:(1-x)\text{SiO}_2$ (molar).

** Parameters taken from Neuville and Richet (1991). Wox corresponds to $x\text{CaSiO}_3:(100-x)\text{MgSiO}_3$ (molar). Gr_x corresponds to $x\text{Ca}_2\text{Al}_2\text{Si}_2\text{O}_{12}:(100-x)\text{Mg}_2\text{Al}_2\text{Si}_2\text{O}_{12}$ (molar).

†† Parameters calculated using the viscosity data summarized by Bansal and Doremus (1986), and the model of Richet and Bottinga (1985) for values of C_p^{cont} . Na_xCS_y corresponds to $x\text{Na}_2\text{O}:(100-x-y)\text{CaO}:y\text{SiO}_2$ (molar).

over whether the latter measurements represent structurally relaxed, equilibrium viscosities. If the low-temperature data of Hetherington et al. (1964) are used rather than those of Urbain et al. (1982), a better fit to the viscosity curve is obtained and a value of 19 600 is calculated for $B_e/S_{\alpha}(T_g)$ (Table 1).

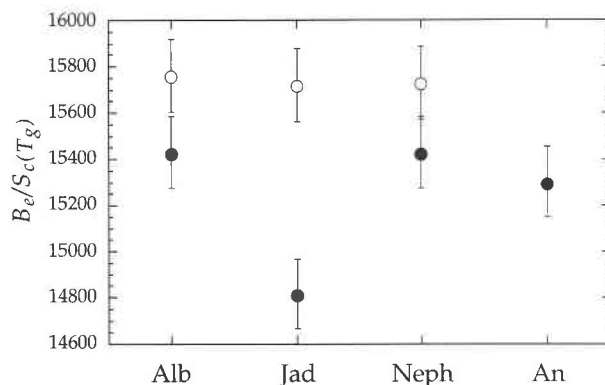


FIGURE 2. Variation of $B_e/S_{\alpha}(T_g)$ for “fully polymerized” aluminosilicates. Alb = NaAlSi₃O₈; Jad = NaAlSi₂O₆; Neph = NaAlSiO₄; An = CaAl₂Si₂O₈. Filled symbols calculated using viscosity data for compositions exactly along the join SiO₂-NaAlSiO₄. Open symbols calculated using viscosity data for compositions inferred to contain no non-bridging O atoms (see text for details). Error bar represents $\pm 1\%$.

Other aluminosilicate compositions, which are generally considered to consist of a fully polymerized network of silicate and aluminate tetrahedra, include albite, jadeite, nepheline, anorthite and orthoclase. Using the A-G equations given by Toplis et al. (1997a) for the join SiO₂-NaAlSiO₄ and by Richet (1984) for anorthite (summarized in Table 1), it is found that four of these compositions show similar values of $B_e/S_{\alpha}(T_g)$ in the range 14 800–15 400 (Fig. 2). However, it has recently been suggested that, at least for compositions on the join SiO₂-NaAlSiO₄, melts along the subaluminous join may contain some non-bridging O (NBO) atoms and that the fully polymerized case actually occurs slightly within the peraluminous field (Toplis et al. 1997a, 1997b). The latter authors provide viscosity data for compositions that are close to the inferred fully polymerized state. If these viscosity data are used, and it is assumed that changes in the configurational heat capacity are negligible over the small compositional range from the metaluminous join into the peraluminous field (an assumption supported by the calorimetric data of Richet 1982), then within $\leq \pm 1\%$ a constant value for the ratio $B_e/S_{\alpha}(T_g)$ (15×750) is calculated (Fig. 2). It is possible that anorthite melt also contains some NBO (Toplis and Dingwell 1996; Stebbins and Xu 1997) and that the corresponding “fully polymerized” composition may also have a value of $B_e/S_{\alpha}(T_g)$ higher than that shown in Figure 2. Viscosity data for orthoclase unfortunately are lacking at temperatures close to the glass transition, but Richet (1984) reported that the A-G parameters that best fit the available viscosity data provide a value for $B_e/S_{\alpha}(T_g)$ of 16 200, which is close to values for the other aluminosilicate network liquids discussed above.

The join SiO₂-Na₂O

Melts in the system SiO₂-Na₂O are structurally different from the fully polymerized network liquids described

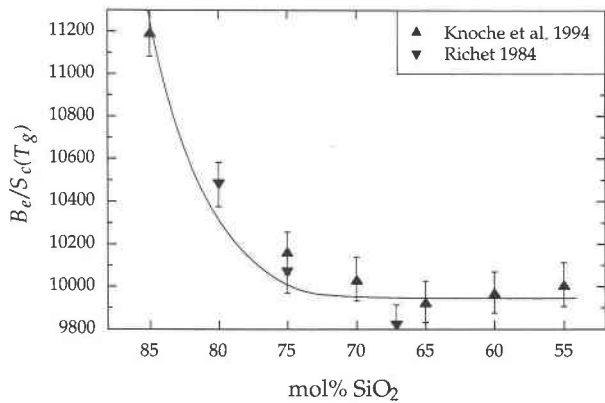


FIGURE 3. Variation of $B_e/S_c(T_g)$ along the join $\text{SiO}_2\text{-Na}_2\text{O}$. The solid line was calculated using Equations 13 and 17, and values for $B_e/S_c(T_g)_{\text{SiO}_2} = 19\,600$; $B_e/S_c(T_g)_{\text{NBO-Na}} = 9\,950$; and $\phi_{\text{SiO}_2}/\phi_{\text{NBO-Na}} = 0.33$ (see text for details). Error bar represents $\pm 1\%$.

above in that sodium occupies network modifying roles, thus non-bridging O atoms are present. Combining A-G parameters for the three sodium silicates reported in Richet (1984) with those calculated from the more recent viscosity data of Knoche et al. (1994) (Table 1), it is found that the calculated values of $B_e/S_c(T_g)$ show an extremely well-defined variation as a function of SiO_2 content (Fig. 3). At silica contents in the range 67–55 mol%, $B_e/S_c(T_g)$ shows an approximately constant value close to 10 000, while at higher SiO_2 contents its value rises in a non-linear, but smooth fashion toward that defined for pure SiO_2 (16 700–19 600).

Alkali tetrasilicates

In contrast to the join $\text{SiO}_2\text{-Na}_2\text{O}$ where the state of polymerization varies as a function of composition, that of the alkali tetrasilicates ($\text{M}_2\text{Si}_4\text{O}_9$, where M is Li, Na, K, Rb, Cs) is constant, the only variable being the nature of the monovalent cation. Although the relevant viscosity and calorimetric data are not available for all of these compositions, the values of their glass transition temperatures (Mazurin et al. 1987) may be used to estimate values of $B_e/S_c(T_g)$ using Equation 11 (assuming that all alkali tetrasilicates have the same value of A_e as that determined for $\text{Na}_2\text{Si}_4\text{O}_9$, as will be justified below). In this case it is found that the ratio $B_e/S_c(T_g)$ increases from Li to Cs. Furthermore, this increase is found to be a linear function of the radius of the cation in octahedral coordination (Fig. 4).

Alkaline earth silicates and aluminosilicates

In contrast to the systems considered above, which contain a single network modifying cation, the two joins $\text{CaSiO}_3\text{-MgSiO}_3$ and $\text{Ca}_3\text{Al}_2\text{Si}_3\text{O}_{12}\text{-Mg}_3\text{Al}_2\text{Si}_3\text{O}_{12}$ studied by Neuville and Richet (1991) provide important data for systems containing two different network modifying cations. Using the values for the Adam-Gibbs parameters extracted by Neuville and Richet (1991) it is observed that despite the non-linear variations of B_e and $S_c(T_g)$

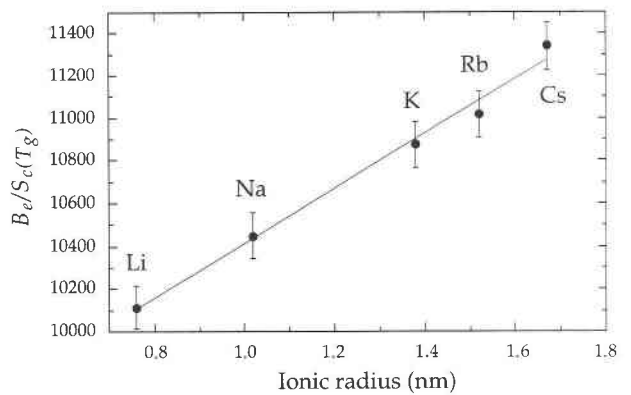


FIGURE 4. Variation of $B_e/S_c(T_g)$ for alkali tetrasilicates ($\text{M}_2\text{Si}_4\text{O}_9$) as a function of ionic radius in octahedral coordination (values taken from Shannon 1976). Error bar represents $\pm 1\%$.

across both of these joins (Fig. 1) the ratio of these two parameters is constant to within $\pm 2\%$ (Fig. 5a). In addition, the values of $B_e/S_c(T_g)$ for the pyroxene and the garnet compositions are very similar in magnitude (and sim-

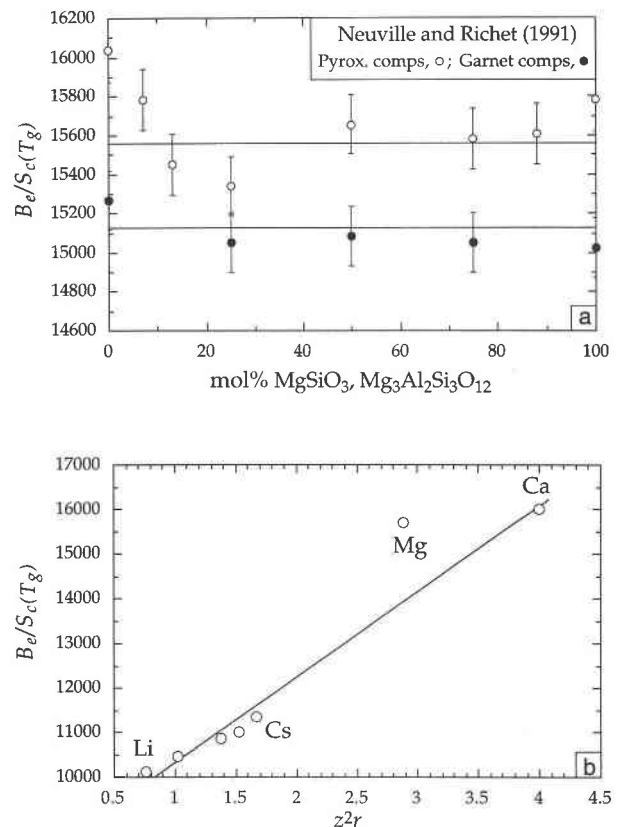


FIGURE 5. (a) Variation of $B_e/S_c(T_g)$ along the joins $\text{CaSiO}_3\text{-MgSiO}_3$ (pyroxenes) and $\text{Ca}_3\text{Al}_2\text{Si}_3\text{O}_{12}\text{-Mg}_3\text{Al}_2\text{Si}_3\text{O}_{12}$ (garnets). An error bar of $\pm 1\%$ is shown. (b) Values of $B_e/S_c(T_g)$ for Ca- and Mg-bearing compositions compared with alkali-bearing compositions as a function of z^2r (z = ionic charge; r = ionic radius). See text for details.

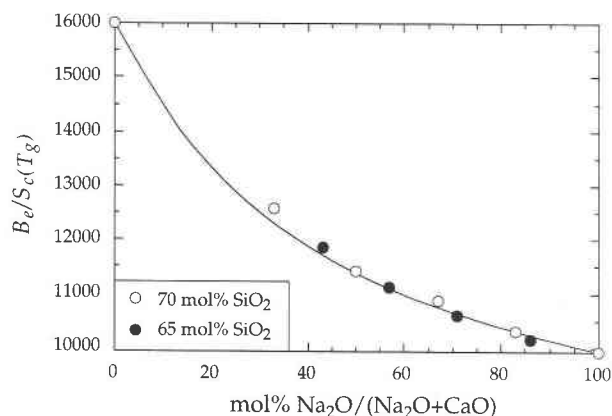


FIGURE 6. Variation of $B_e/S_c(T_g)$ along the 65 and 70 mol% SiO_2 isopleths in the system $\text{Na}_2\text{O}-\text{CaO}-\text{SiO}_2$. The solid line was calculated using Equations 13 and 16, and values of $B_e/S_c(T_g)_{\text{NBO-Ca}} = 16\,000$; $B_e/S_c(T_g)_{\text{NBO-Ca}} = 9950$; and $\{\phi_{\text{NBO-Na}}/\phi_{\text{NBO-Ca}}\} = 0.31$ (see text for details).

ilar to that of anorthite composition) although the ratio $B_e/S_c(T_g)$ of the aluminosilicate garnet compositions is consistently slightly lower than that of the pyroxenes. Furthermore, comparison of the values of $B_e/S_c(T_g)$ for the depolymerized compositions containing the divalent cations Mg and Ca with those for the alkali tetrasilicates (Fig. 5b), shows that the value for CaSiO_3 lies close to the extrapolation of the alkali data when plotted as a function of z^2r , where z is the cationic charge and r is the cationic radius. The significance of this observation will be discussed below.

Mixed alkali-alkaline earth silicates

Viscosity data for the system $\text{Na}_2\text{O}-\text{CaO}-\text{SiO}_2$ (data taken from compilation of Bansal and Doremus 1986) provide an opportunity to study the variation of $B_e/S_c(T_g)$ in a system containing two different network-modifying cations, whose end-member values of $B_e/S_c(T_g)$ are significantly different. Along the 65 and 70 mol% SiO_2 isopleths in this system, values for $B_e/S_c(T_g)$ vary as a smooth function of Na/Ca between the limits defined by the Ca and Na end-members (Fig. 6). However, although intermediate compositions show values in the range defined by those of the end-members, they do not simply lie on an ideal mixing line between them, but below it. Identical behavior is also observed on joins at 75 and 60 mol% SiO_2 .

VISCOUS FLOW MECHANISMS

It is clear from Figures 2–6 that the ratio $B_e/S_c(T_g)$ shows relatively simple variations as a function of composition, which may be parameterized. Before attempting such a parameterization, it is instructive to assess to what extent the observed variations in $B_e/S_c(T_g)$ may be explained in terms of the two parameters, $\Delta\mu$ and $z^*(T_g)$ (Eq. 10). Although there is no way to estimate the magnitude or compositional dependence of the second of

these terms, we know that the height of the potential energy barrier ($\Delta\mu$) is controlled by the microscopic mechanism(s) responsible for viscous flow. Our understanding of such mechanisms has improved greatly in recent years, due in large part to elegant demonstrations by NMR spectroscopy of the close link between viscous relaxation times and oxygen bond-breaking and reforming events (Farnan and Stebbins 1994; Stebbins et al. 1995). It is now possible to predict qualitatively how $\Delta\mu$ will vary as a function of composition, and thus to assess whether $\Delta\mu$ is a major or minor factor contributing to observed variations in $B_e/S_c(T_g)$.

COMPOSITIONS CONTAINING A SINGLE NETWORK-MODIFYING CATION

There is now a general consensus that in melts containing abundant NBO, the primary mode of viscous flow occurs through the attack of a tetrahedral Si or Al cation by an NBO to produce temporarily a high-coordinate network former (see Stebbins 1995). The presence of such high-coordinate species not only is predicted from molecular dynamics (MD) simulations (see Poole et al. 1995), but also has been observed directly, even in glasses quenched at one atmosphere pressure (Stebbins 1991).

If one considers such a process in detail, it is clear that the activation energy required for the formation of a high-coordinate network former from interaction with an NBO will consist of two distinct contributions. The first is that required to remove the network-modifying cation from the vicinity of the O with which it is associated (its NBO). The second is the energy required to attach this “free” NBO to the coordination shell of the network-forming Si or Al to form the high-coordinate species. Although the magnitude of the second contribution should be more or less independent of the nature of the network-modifying cation, the first will be a function of the identity of that cation and may be expected to be inversely correlated to the self-diffusivity of that cation in that melt. LaTourrette et al. (1996) have shown recently that the self-diffusivities of Mg and Ca in a depolymerized composition at temperatures between 1623–1773 K are identical within error. This observation, and the very similar values of $B_e/S_c(T_g)$ for CaSiO_3 and MgSiO_3 (Fig. 5), suggest that $\Delta\mu$ could be the dominant factor controlling the ratio $B_e/S_c(T_g)$. Hofmann (1980) and more recently LaTourrette and Wasserburg (1997) have shown that for a wider range of cations self-diffusivity in depolymerized melts is, to a first approximation, a linear function of z^2r , where z is the charge and r is the cationic radius (although the self-diffusivity data for Mg and Ca show that this general trend is not always followed). The observed linear variation of $B_e/S_c(T_g)$ as a function of cationic radius for the alkali tetrasilicates (Fig. 3), and the fact that the value of $B_e/S_c(T_g)$ for CaSiO_3 also lies near this trend when plotted as a function of z^2r (Fig. 5b), suggest further that $B_e/S_c(T_g)$ is proportional to the self-diffusivity of network-modifying cations, and that $\Delta\mu$ is the dominant factor controlling the ratio. A z^2r dependency of cationic self-diffusion thus

provides an explanation for the significantly higher values of $B_e/S_c(T_g)$ for melts consisting primarily of divalent cations compared with monovalent cations.

Compositions containing two different network-modifying cations

In a melt where more than one mechanism is active, the average energy barrier to viscous flow ($\Delta\mu_{\text{avg}}$) will be controlled by two factors: (1) the energy barrier associated with each individual mechanism, and (2) the relative proportions of each mechanism. This may be summarized by the equation:

$$\Delta\mu_{\text{avg}} = \sum_i \Psi_i \Delta\mu_i \quad (12)$$

where Ψ_i is the fraction of mechanism i operating, and $\Delta\mu_i$ is the energy barrier of mechanism, i . For example, in a depolymerized melt containing two different network-modifying cations, there will be two potential mechanisms of viscous flow (one for each cation), each having its own energy barrier. If the two end-member energies are the same, then one would expect no variation in the average energy barrier for intermediate compositions (Eq. 12). However, in cases where the two end-member mechanisms have significantly different energy barriers, then we may expect a smooth variation of the average barrier from one end-member to the other as a function of composition. The exact form of this variation will depend on the relative frequencies of the two end-member mechanisms, which may depend not only on the relative mole fractions of participating species in the melt but also on the magnitude of the end-member energy barriers, with lower energy routes possibly favored over higher energy routes.

The variations of $B_e/S_c(T_g)$ described above show exactly these features. For example, along the two Ca-Mg binary joins where the end-member values of $B_e/S_c(T_g)$ are very similar (Fig. 5a), there is almost no variation of $B_e/S_c(T_g)$ for intermediate compositions, whereas along the Na-Ca binary joins (Fig. 6) there is a smooth variation between the two end-member values with a clear deviation to values lower than the 1:1 mixing line for intermediate compositions. Such data are also consistent with $\Delta\mu$ being the dominant factor affecting the ratio $B_e/S_c(T_g)$.

Compositions containing no network-modifying cations

It is clear that in silicate melts containing no NBOs, viscous flow cannot take place through the mechanism described above. McMillan et al. (1994) recently have discussed and proposed viscous flow mechanisms in pure SiO_2 and fully polymerized aluminosilicate melts. In the case of pure silica, those authors proposed that it was necessary to break a strong Si-O-Si bond, whereas in the case of a fully polymerized aluminosilicate it was proposed that a weaker Si-O-Al bond may be broken forming a threefold-coordinated O atom and fivefold-coordinated Al during the viscous flow event. A similar process has been proposed recently for fully polymerized aluminosilicates by Toplis et al. (1997b), who suggested that mi-

gration of a charge-balancing cation away from its Al may lead to the disruption of an Si-O-Al bond to form a threefold-coordinated O atom (tricluster) without the need to form a high-coordinate Al. In either case, one may expect the energy barrier for viscous flow in silica to be higher than that in aluminosilicates, as observed (Table 1). Viscous flow in fully polymerized aluminosilicates that contain a single charge-balancing cation will be dominated by a flow mechanism involving aluminate tetrahedra, and therefore similar for all compositions, at least in the range 75–50 mol% SiO_2 where aluminate tetrahedra are abundant, as observed for albite, jadeite, and nepheline compositions (Fig. 2). In addition, it is noteworthy that $B_e/S_c(T_g)$ is greatest for orthoclase composition and smallest for anorthite composition (Table 1), which is in qualitative agreement with expected variations in the strength of the Al-O-Si bond (e.g., Seifert et al. 1982). Therefore, these observations are also consistent with a dominant role for $\Delta\mu$ in controlling $B_e/S_c(T_g)$.

Compositions of variable polymerization

In contrast to the joins described above, melts along the $\text{Na}_2\text{O-SiO}_2$ binary vary from highly depolymerized to fully polymerized. In depolymerized melts where every silicate tetrahedron is adjacent to a tetrahedron containing at least one NBO the formation of fivefold-coordinated Si through interaction with an NBO should be the unique mechanism of viscous flow. This should be the case for compositions with silica contents less than 67 mol%, (if the minor effect of the disproportionation reaction $2\text{Q}^3 = \text{Q}^2 + \text{Q}^4$ (e.g., Mysen 1995) is ignored), and thus the energy barrier to viscous flow may be expected to be relatively constant in this range. At higher silica contents, however, an increasing proportion of viscous flow events may occur through the mechanism that operates in pure silica (which involves silicate tetrahedra with no NBO, i.e., Q^4 species). Given that the energy barrier for a mechanism involving Q^4 species is considerably higher than that involving NBOs attached to Na, an increase in the average height of the energy barrier to viscous flow may be expected as the silica content increases from 67–100 mol%. It is clear that the values of $B_e/S_c(T_g)$ along the binary join $\text{SiO}_2\text{-Na}_2\text{O}$ show exactly this behavior, with an approximately constant value at SiO_2 contents less than 67 mol%, and a change to increasing values at higher SiO_2 contents, implying that the variation of $B_e/S_c(T_g)$ along this join of variable polymerization may also be explained by a dominant role for $\Delta\mu$.

Variations in $z^*(T_g)$

As shown above, variations of $B_e/S_c(T_g)$ for a wide range of silicate compositions show the same features that one would predict qualitatively for variations of the potential energy barrier to viscous flow. Based on such an observation it is tempting to postulate that $z^*(T_g)$ may be a constant for all silicate melts at their glass transition (when defined at a constant cooling rate), and thus that z^* , the size of the rearranging regions, is the factor that

defines the calorimetric glass transition. Indeed, Bottinga and Richet (1996), in their recent discussion of the Adam-Gibbs theory, quoted the results of independent studies by Duval et al. (1990), Sokolov et al. (1993), and Moynihan and Schroeder (1993) that provide evidence for discrete domains in SiO_2 and B_2O_3 glasses whose physical size was extremely similar in both cases. Such evidence is therefore also compatible with the idea that $z^*(T_g)$ may be a constant, at least for network liquids such as silicate melts. The only surprising implication of such a conclusion is that the energy barrier for viscous flow in fully polymerized aluminosilicates such as albite or anorthite is very similar to that of a highly depolymerized composition such as CaSiO_3 . However, as discussed above, the self-diffusion data suggest a general z^2r dependence of self-diffusivity for network-modifying cations that may account for the relatively high values of $\Delta\mu$ for the divalent cations. Furthermore, if viscous flow in fully polymerized compositions requires only the breaking of an Al-O-Si bond, without the formation of a high-coordinate Al (Toplis et al. 1997b), then it is possible that the energy required is about the same order of magnitude as that in depolymerized Ca-bearing compositions. It is also of note that the intermediate composition $\text{Ca}_3\text{Al}_2\text{Si}_3\text{O}_{12}$ has a value of $B_e/S_c(T_g)$ identical to that of the two end-members CaSiO_3 and $\text{CaAl}_2\text{Si}_2\text{O}_8$, consistent with Equation 12.

PARAMETERIZATION

$B_e/S_c(T_g)$

Although the present analysis cannot prove that $z^*(T_g)$ is a constant for all silicate glasses, the compositional variations of $B_e/S_c(T_g)$ presented above may be explained solely in terms of $\Delta\mu$, which is consistent with such a postulate. Furthermore, making this assumption allows us to parameterize values of $B_e/S_c(T_g)$ within the framework of a physical model that may be checked and extended to more complex compositions as further data become available. If the ratio $B_e/S_c(T_g)$ is directly proportional to $\Delta\mu$, then each viscous flow mechanism, i , has an associated value of $B_e/S_c(T_g)$, thus:

$$[B_e/S_c(T_g)]_{\text{avg}} = \sum_i \Psi_i [B_e/S_c(T_g)]_i \quad (13)$$

where $[B_e/S_c(T_g)]_{\text{avg}}$ is the average $B_e/S_c(T_g)$ of a given composition, and Ψ_i is the fraction of mechanism i operating. Even based on the available data, we can estimate the magnitude of $B_e/S_c(T_g)_i$ for almost all the end-member mechanisms likely to occur in geological melts with the important exception of those involving iron. These are: (1) that occurring in SiO_2 [preferred value of $B_e/S_c(T_g) = 19\,600$]; (2) that occurring in fully polymerized aluminosilicates (15 700); and (3) one mechanism associated with each network-modifying cation (NBO-Na = 9950, NBO-K = 10 300, NBO-Mg = 15 800, and NBO-Ca = 16 000).

Once the end-member values of $B_e/S_c(T_g)_i$ have been defined, a method for calculating the relative probabilities (Ψ_i) is required for compositions in which more than one mechanism is operating. In a general case, the absolute

probability of a given mechanism (ϕ_i) may be governed by two terms (Eq. 14).

$$\phi_i = \phi_i \omega_i \quad (14)$$

where ω_i is the physical probability of the necessary components interacting (a function of the mole fractions of the necessary components), and ϕ_i is a weighting factor that increases the relative probability of lower energy mechanisms [in the simplest case ϕ_i may be inversely proportional to $B_e/S_c(T_g)_i$]. Unfortunately, of the data sets presented above, only two may be used to test and calibrate values for Ψ_i , although these cover the two important cases of mixtures of different network-modifying cations (the system $\text{Na}_2\text{O-CaO-SiO}_2$) and a join varying from depolymerized to fully polymerized ($\text{SiO}_2\text{-Na}_2\text{O}$).

In the case of melts in the system $\text{CaO-Na}_2\text{O-SiO}_2$, the two flow mechanisms are: (1) an NBO attached to Na interacting with a silicate tetrahedron and (2) an NBO attached to Ca interacting with a silicate tetrahedron. The physical probabilities (ω_i) are $\{X[\text{NBO}_{\text{Na}}] \cdot X[\text{Si}]\}$ and $\{X[\text{NBO}_{\text{Ca}}] \cdot X[\text{Si}]\}$, respectively, where $X[\text{NBO}_{\text{Na}}]$ and $X[\text{NBO}_{\text{Ca}}]$ are the number of non-bridging O atoms attached to Na and Ca, respectively, and $X[\text{Si}]$ is the number of Si atoms. Therefore, the fraction of flow events occurring through NBOs attached to Na is:

$$\Psi_{\text{NBO-Na}} = (\phi_{\text{NBO-Na}} \{X[\text{NBO}_{\text{Na}}] \cdot X[\text{Si}]\}) / (\phi_{\text{NBO-Na}} \{X[\text{NBO}_{\text{Na}}] \cdot X[\text{Si}]\} + \phi_{\text{NBO-Ca}} \{X[\text{NBO}_{\text{Ca}}] \cdot X[\text{Si}]\}) \quad (15)$$

which may be simplified to:

$$\Psi_{\text{NBO-Na}} = X[\text{NBO}_{\text{Na}}] / (X[\text{NBO}_{\text{Na}}] + \{\phi_{\text{NBO-Ca}} / \phi_{\text{NBO-Na}}\} X[\text{NBO}_{\text{Ca}}]) \quad (16)$$

If the data for the Ca-Na join at 70 mol% SiO_2 are fit to Equations 13 and 16, a value for the ratio $\{\phi_{\text{NBO-Na}} / \phi_{\text{NBO-Ca}}\}$ of 0.36 is found to reproduce all of the intermediate data points to within 1%. Such a value for $\phi_{\text{NBO-Na}} / \phi_{\text{NBO-Ca}}$ is considerably less than the $B_e/S_c(T_g)$ ratio of the end-members (~ 0.63), suggesting that ϕ_i may not simply be inversely proportional to $B_e/S_c(T_g)_i$. However, another possibility is that only one of the two NBOs attached to divalent cations is available for viscous flow. In this case, the value $X[\text{NBO}_{\text{Ca}}]$ would be half the value expected, giving rise to an apparent ratio $\{\phi_{\text{NBO-Na}} / \phi_{\text{NBO-Ca}}\}$ of 0.31. If a value for $\{\phi_{\text{NBO-Na}} / \phi_{\text{NBO-Ca}}\}$ of 0.31 is assumed, and the variation of $B_e/S_c(T_g)$ on the join Na-Ca is calculated using Equations 13 and 16, it is found that the data points lie very close to the predicted curve, as shown in Figure 6. Additional data on different pseudo-binary joins involving monovalent and divalent cations clearly are required to constrain the dependence of ratios of ϕ_i on the values of $B_e/S_c(T_g)$ of the end-members and the valence state of the cations involved.

In the case of the system $\text{SiO}_2\text{-Na}_2\text{O}$, the two potential mechanisms of viscous flow are: (1) interaction of an NBO and a silicate tetrahedron and (2) that occurring in pure SiO_2 , which may involve 4Q^4 species (McMillan et

al. 1994). The physical probabilities may therefore be $\{X[\text{NBO}_{\text{Na}}] \cdot X[\text{Si}]\}$, and $(X[\text{Q}^4])^4$, respectively. In this case the relative probability of the NBO mechanism will be:

$$\Psi_{\text{NBO-Na}} = \frac{\{X[\text{NBO}_{\text{Na}}] \cdot X[\text{Si}]\}}{\{X[\text{NBO}_{\text{Na}}] \cdot X[\text{Si}]\} + \{(\phi_{\text{SiO}_2}/\phi_{\text{NBO-Na}}) \cdot (X[\text{Q}^4])^4\}} \quad (17)$$

where ϕ_{SiO_2} is the weighting factor of the mechanism operating in pure SiO_2 (the Q^4 mechanism). It is clear that the $(X[\text{Q}^4])^4$ term in Equation 17 will result in a highly non-linear variation of $B_e/S_c(T_g)_{\text{avg}}$ along this join as indeed observed (Fig. 3). If the data along the join SiO_2 - Na_2O are fit to Equations 13 and 17 and $\phi_{\text{SiO}_2}/\phi_{\text{NBO-Na}}$ is considered a free variable, the values of $B_e/S_c(T_g)$ along this join may be reproduced rather well (as shown in Fig. 3). The quality of the fit is similar using end-member values of $B_e/S_c(T_g)$ for SiO_2 of 16700 or 19600, and the value of $\phi_{\text{SiO}_2}/\phi_{\text{NBO-Na}}$ is approximately 0.66 times the ratio of the end-member values of $B_e/S_c(T_g)$ in each case.

These limited data show that parameterization within the framework of Equations 13 and 14 successfully describes the variation of $B_e/S_c(T_g)$ on joins where two different viscous flow mechanisms are operating, giving hope that values of $B_e/S_c(T_g)$ of more complex compositions may also be parameterized within this framework.

A_e and the prediction of T_g

To estimate glass transition temperatures it is also necessary to predict the magnitude of the A_e term (Eq. 11). As shown in Table 1, absolute values of A_e for different compositions show a restricted range from -1.5 and -3.7 , which may be expected based on Equation 6. Therefore, to a first approximation, a value of -2.6 ± 1 may be used, which corresponds to an error of ± 50 – 70 K in the calculated values of T_g for typical silicate melts. However, it is clear that if detailed knowledge of T_g is desired then a better estimate of A_e is required. Indeed, it is interesting to note that the ratio $B_e/S_c(T_g)$ is constant along the join CaSiO_3 - MgSiO_3 , therefore, the pronounced minimum in glass transition temperature along this join (Neuville and Richet 1991) must be attributed to variations in A_e alone. Thus, in this case, and maybe in other cases such as the Na-K mixed alkali joins discussed by Richet (1984), variations in the glass transition temperature are not caused directly by variations in $S_c(T_g)$ (i.e., Eq. 1) but indirectly through the A_e term (see Eq. 6, Fig. 1). However, if all the available data are considered together, there is no single equation that relates A_e to either $S_c(T_g)$ or B_e (Fig. 7a and b). One possible explanation for this dispersion is that A_e is related to some molar property of the melt, but which does not correspond to one gram formula weight. Toplis et al. (1997a) have suggested that $S_c(T_g)$ may be linked to mixing of tetrahedral sites. If the variation of A_e is considered as a function of $B_e/[\text{tetrahedra}]$ (i.e., Si + Al), a very satisfactory linear correlation is observed (Fig. 7c). Although the physical significance of this empirical correlation remains to be explained in detail, it may be used to recover values of A_e for the wide

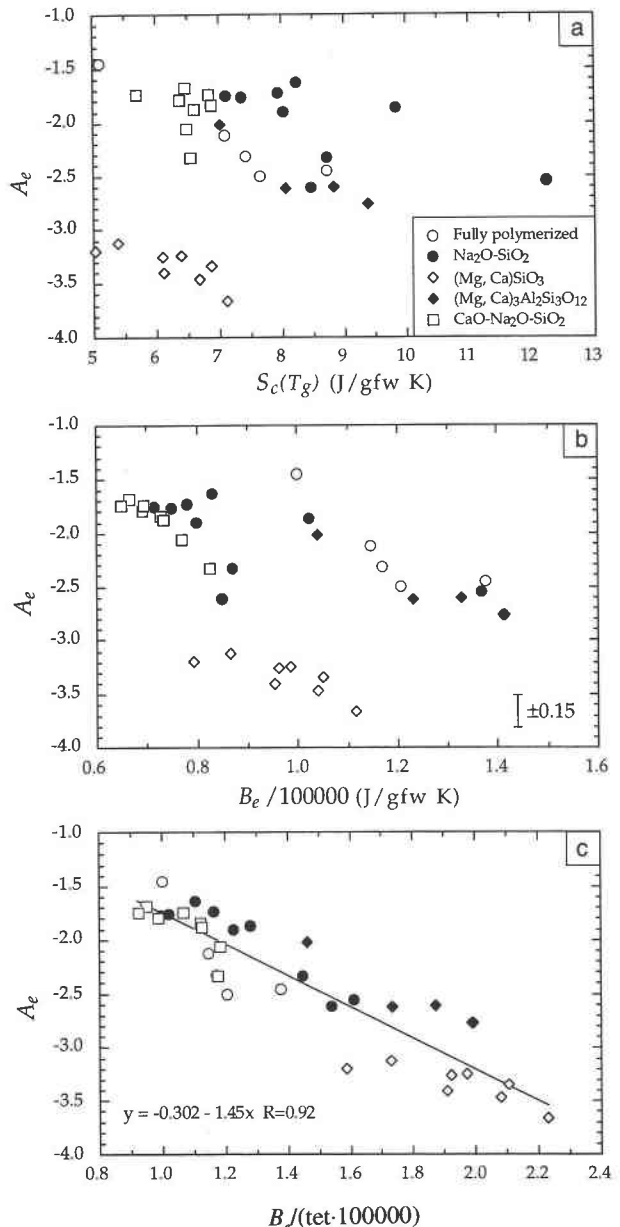


FIGURE 7. Variation of A_e for different compositions as a function of (a) $S_c(T_g)$; (b) B_e ; and (c) $B_e/\text{tetrahedron}$ (Si + Al). Values are in gram formula weight. The error in individual values of A_e is approximately ± 0.15 . The equation shown in (c) recovers values to within ± 0.3 .

range of compositions of very variable polymerization described above to within ± 0.3 , which corresponds to an error in calculated glass transition temperature of approximately ± 15 – 20 K.

Prediction of viscosity

Reliable estimation of the glass transition temperature is clearly an important step toward the prediction of viscosity at higher temperatures. However, the present anal-

ysis cannot be used to predict the entire viscosity curve using the Adam-Gibbs theory because the absolute values of B_c and $S_c(T_g)$ are not known, but only their ratio. Once a robust model for the calculation of configurational entropy at the glass transition as a function of composition becomes available, the absolute values of B_c and $S_c(T_g)$ may be assessed and combined with values for C_p^{conf} (Richtet and Bottinga 1985, 1986) to calculate the entire viscosity curve (Eqs. 1 and 2). In the meantime, the value of T_g may be combined with estimates of viscosity in the low-viscosity range ($10\text{--}10^5$ Pa·s) using models such as those of Bottinga and Weill (1972) or Shaw (1972). At least two high-temperature viscosities (and thus the gradient of the log viscosity-inverse temperature curve at high temperature) and the glass transition temperature may be fit to the commonly used Tamann-Vogel-Fulcher (TVF) equation (an equation that is found to reproduce closely the experimentally determined viscosity curves over large temperature ranges) to estimate the whole viscosity curve. Such a procedure will indicate the degree of departure from Arrhenian behavior, thus representing a significant improvement on these existing models.

SUMMARY

The results presented here indicate that the ratio $B_c/S_c(T_g)$ for a wide range of simple silicate compositions shows variations as a function of composition that are directly proportional to those which one may expect qualitatively for variations in the height of the potential energy barrier to viscous flow. However, it is clear that much work remains to be done to verify the underlying assumptions (i.e., the constancy of z^* at the glass transition) and to extend the model to compositions of geological interest. For example, end-member values for $B_c/S_c(T_g)$ for flow mechanisms involving Fe need to be defined, although the case of Fe is complicated by the fact that it may occur in the divalent or trivalent state, as well as the fact that the structural role of Fe^{3+} may also be a function of the redox conditions (Virgo and Mysen 1985). It is also possible that the dependence of $B_c/S_c(T_g)$ on z^*r (Fig. 3) observed for the monovalent cations may be extrapolated to H, thus providing an estimate of the values of $B_c/S_c(T_g)$ in hydrous depolymerized melts. It is clear that the study of pseudobinary joins containing combinations of two different network modifiers is required to constrain how ϕ_i varies as a function of composition. Furthermore, an essential extension of the model to compositions of geological interest is to consider intermediate joins where both network modifiers and aluminate tetrahedra are abundant (e.g., $\text{Na}_2\text{Si}_2\text{O}_5\text{--NaAlSi}_2\text{O}_6$). If such studies are found to support the validity of the present parameterization then other elements whose structural role is known to be more complex (e.g., P, B, Ti) may be studied. In these cases variations of $B_c/S_c(T_g)$ may provide evidence of viscous flow mechanisms involving these cations.

ACKNOWLEDGMENTS

A Human Capital and Mobility grant from the European Union is acknowledged during the early stages of this work. Discussions with B. Poe, J. Mungall, and G. Libourel are appreciated as well as helpful reviews by J. Tangeman and B. Mysen.

REFERENCES CITED

- Adam, G. and Gibbs, J.H. (1965) On the temperature dependence of cooperative relaxation properties in glass-forming liquids. *Journal of Chemical Physics*, 43, 139–146.
- Bansal, N.P. and Doremus, R.H. (1986) *Handbook of glass properties*, 680 p. Academic Press, New York.
- Bottinga, Y. and Weill, D.F. (1972) The viscosity of magmatic liquids: a model for calculation. *American Journal of Science*, 272, 438–475.
- Bottinga, Y. and Richet, P. (1996) Silicate melt structural relaxation: rheology, kinetics, and Adam-Gibbs theory. *Chemical Geology*, 128, 129–141.
- Bottinga, Y., Richet, P., and Sipp, A. (1995) Viscosity regimes of homogeneous silicate melts. *American Mineralogist*, 80, 305–318.
- Cohen, M.H. and Grest, G.S. (1979) Liquid-glass transition, a free volume approach. *Physical Review B*, 20, 1077–1098.
- Dingwell, D.B. and Webb, S.L. (1989) Structural relaxation on silicate melts and non-Newtonian melt rheology in geologic processes. *Physics and Chemistry of Minerals*, 16, 508–516.
- (1990) Relaxation in silicate melts. *European Journal of Mineralogy*, 2, 427–449.
- Duval, E., Boukenter, A., and Achibat, T. (1990) Vibrational dynamics and the structure of glasses. *Journal of Physics of Condensed Matter*, 2, 10227–10234.
- Farnan, I. and Stebbins, J.F. (1994) The nature of the glass transition in a silica-rich oxide melt. *Science*, 265, 1206–1209.
- Götze, W. (1991) Aspects of structural glass transitions. In: J.P. Hansen, D. Levesque, and J. Zin-Justin, Eds., *Liquids, Freezing, and Glass Transition*, Volume 1, p. 292–503. Elsevier, Amsterdam.
- Hetherington, G., Jack, K.H., and Kennedy, J.C. (1964) The viscosity of vitreous silica. *Physics and Chemistry of Glasses*, 5, 130–136.
- Hofmann, A.W. (1980) Diffusion in natural silicate melts: A critical review. In R.B. Hargraves, Ed., *Physics of Magmatic Processes*, p. 385–417. Princeton University Press, Princeton, New Jersey.
- Hummel, W. and Arndt, J. (1985) Variation of viscosity with temperature and composition in the plagioclase system. *Contributions to Mineralogy and Petrology*, 90, 83–92.
- Knoche, R., Dingwell, D.B., Seifert, F.A., and Webb, S.L. (1994) Non-linear properties of supercooled liquids in the system $\text{Na}_2\text{O--SiO}_2$. *Chemical Geology*, 116, 1–16.
- LaTourrette, T. and Wasserburg, G.J. (1997) Self diffusion of europium, neodymium, thorium, and uranium in a haplobasaltic melt: The effect of oxygen fugacity and the relationship to melt structure. *Geochimica et Cosmochimica Acta*, 61, 755–764.
- LaTourrette, T., Fahey, A.J., and Wasserburg, G.J. (1996) Self diffusion of Mg, Ca, Ba, Nd, Yb, Ti, Zr, and U in haplobasaltic melt. *Geochimica et Cosmochimica Acta*, 60, 1329–1340.
- Mazurin, O.V., Streltsina, M.V., and Shvaiko-shvaikovskaya, T.P. (1987) *Handbook of glass data. Part C: Ternary silicate glasses*. *Physical Sciences Data* 15, pp 1110, Elsevier.
- McMillan, P.F., Poe, B.T., Gillet, P., and Reynard, B. (1994) A study of SiO_2 glass and supercooled liquid to 1950K via high temperature Raman spectroscopy. *Geochimica et Cosmochimica Acta*, 58, 3653–3664.
- Moynihn, C.T. and Schroeder, J. (1993) Non-exponential relaxation, anomalous light scattering and nanoscale inhomogeneities in glass forming liquids. *Journal of Non-Crystalline Solids*, 160, 52–59.
- Mysen, B.O. (1995) Experimental, in-situ, high temperature studies of properties and structure of silicate melts relevant to magmatic temperatures. *European Journal of Mineralogy*, 7, 745–766.
- Neuvill, D.R. and Richet, P. (1991) Viscosity and mixing in molten (Ca, Mg) pyroxenes and garnets. *Geochimica et Cosmochimica Acta*, 55, 1011–1019.
- Poole, P.H., McMillan, P.F., and Wolf, G. (1995) Computer simulations of

- silicate melts. In Mineralogical Society of America Reviews in Mineralogy, 32, 563–616.
- Putnis, A. (1992) Introduction to the mineral sciences, 457 p. Cambridge University Press, U.K.
- Richet, P. (1982) Propriétés thermodynamiques des silicates fondus, 322 p. Thesis, Université de Paris VII, Paris.
- (1984) Viscosity and configurational entropy of silicate melts. *Geochimica et Cosmochimica Acta*, 48, 471–483.
- Richet, P. and Bottinga, Y. (1985) Heat capacity of aluminum-free liquid silicates. *Geochimica et Cosmochimica Acta*, 49, 471–486.
- (1986) Thermochemical properties of silicate glasses and liquids: A review. *Reviews in Geophysics*, 24, 1–25.
- (1995) Rheology and configurational entropy of silicate melts. In Mineralogical Society of America Reviews in Mineralogy, 32, 67–93.
- Richet, P., Bottinga, Y., Denielou, L., Petitot, J.P., and Téqui, C. (1982) Thermodynamic properties of quartz, cristobalite and amorphous SiO₂: Drop calorimetry measurements between 1000 and 1800K and a review from 0 to 2000K. *Geochimica et Cosmochimica Acta*, 46, 2639–2658.
- Seifert, F.A., Mysen, B.O., and Virgo, D. (1982) Three-dimensional network structure in the systems SiO₂-NaAlO₂, SiO₂-CaAl₂O₄ and SiO₂-MgAl₂O₄. *American Mineralogist*, 67, 696–711.
- Shannon, R.D. (1976) Revised effective ionic radii and systematic studies of interatomic distances in halides and chalcogenides. *Acta Crystallographa*, A32, 751–767.
- Shaw, H.R. (1972) Viscosities of magmatic silicate liquids: an empirical method of prediction. *American Journal of Science*, 272, 870–893.
- Sokolov, A.P., Kisliuk, A., Soltwisch, M., and Quitmann, D. (1993) Low-energy anomalies of vibrational spectra and medium range order in glasses. *Physica A*, 201, 295–299.
- Stebbins, J.F. (1991) Experimental confirmation of five-coordinated silicon in a silicate glass at 1 atmosphere pressure. *Nature* 351, 638–639.
- (1995) Dynamics and structure of silicate and oxide melts: Nuclear magnetic resonance studies. In Mineralogical Society of America Reviews in Mineralogy, 32, 191–246.
- Stebbins, J.F. and Xu, Z. (1997) NMR evidence for excess non-bridging oxygen in an aluminosilicate glass. *Nature*, 390, 60–62.
- Stebbins, J.F., Sen, S., and Farnan, I. (1995) Silicate species exchange, viscosity, and crystallization in a low-silica melt: In-situ high temperature MAS NMR spectroscopy. *American Mineralogist*, 80, 861–864.
- Tauber, P. and Arndt, J. (1987) The relationship between viscosity and temperature in the system anorthite-diopside. *Chemical Geology*, 62, 71–81.
- Toplis, M.J. and Dingwell, D.B. (1996) Viscosity maxima of melts close to the “charge balanced” join in the system (Na₂O, CaO, MgO)-Al₂O₃-SiO₂: Implications for the structural role of aluminium. *Transactions of the American Geophysical Union*, 77, 848.
- Toplis, M.J., Dingwell, D.B., Hess, K.-U., and Lenci, T. (1997a) Viscosity, fragility, and configurational entropy of melts along the join SiO₂-NaAlSiO₄. *American Mineralogist*, 82, 979–990.
- Toplis, M.J., Dingwell, D.B., and Lenci, T. (1997b) Peraluminous viscosity maxima in Na₂O-Al₂O₃-SiO₂ liquids: The role of triclusters in tectosilicate melts. *Geochimica et Cosmochimica Acta*, 61, 2605–2612.
- Urbain, G., Bottinga, Y., and Richet, P. (1982) Viscosity of silica, silicates and aluminosilicates. *Geochimica et Cosmochimica Acta*, 46, 1061–1071.
- Virgo, D. and Mysen, B.O. (1985) The structural state of iron in oxidized vs. reduced glasses at 1 atm: A ⁵⁷Fe Mössbauer study. *Physics and Chemistry of Minerals*, 12, 65–76.

MANUSCRIPT RECEIVED JUNE 10, 1997

MANUSCRIPT ACCEPTED DECEMBER 4, 1997

PAPER HANDLED BY REBECCA LANGE